Denaturant-Induced Unfolding of the Acetyl-Esterase from *Escherichia coli*†

Pompea Del Vecchio,*,‡ Giuseppe Graziano,§ Vincenzo Granata,‡ Tiziana Farias,‡ Guido Barone,‡ Luigi Mandrich,|| Mosè Rossi,|| and Giuseppe Manco||

Department of Chemistry, University of Naples "Federico II", Via Cintia 45, 80126 Naples, Department of Biological and Environmental Sciences, University of Sannio, Via Port'Arsa 11, 82100 Benevento, Italy, and Institute of Protein Biochemistry, CNR, Via P. Castellino 111, 80131 Naples, Italy

Received August 3, 2004; Revised Manuscript Received September 10, 2004

ABSTRACT: The stability of acetyl-esterase, Aes, from *Escherichia coli* against the denaturing action of urea and guanidine hydrochloride, GuHCl, has been investigated by means of circular dichroism and fluorescence measurements. The urea-induced unfolding curves show a single inflection point at 6.2 M urea, whereas the GuHCl-induced curves show two inflection points at 1.4 and 3.1 M GuHCl. The unfolding process is reversible with both urea and GuHCl. These results, together with similar experimental data on the mutant form V20D-Aes, suggest the presence of two domains in the Aes structure, which unfold more or less independently depending on the denaturant used. This is also supported by a 3D model obtained by homology modeling using the structure of brefeldine as a template. The effect of NaCl on the urea-induced unfolding curves of the enzyme has also been investigated.

It was recently reported that the *ybaC* gene encodes the 36 kDa cytoplasmatic protein Aes[1] (*1*), an acetyl-esterase belonging to the hormone-sensitive lipase, HSL, family (*2*, *3*). The enzyme has received attention because it is involved in the regulation of maltose metabolism in *Escherichia coli*. Specifically, it has been shown that Aes plays a role, by direct protein−protein interaction, in the regulation of MalT, the transcriptional activator of the maltose regulon and the prototype of a new family of transcription factors (*4*). In addition, some of us have found that Aes and the monomeric α-galactosidase from *E. coli* form a noncovalent complex (*5*).

The crystal structures of only three bacterial proteins of the HSL family have been solved up to now: BFAE from *Bacillus subtilis* (*6*), EST2 from *Alicyclobacillus acidocaldarius* (*7*), and AFEST from *Archeoglobus fulgidus* (*8*). In the case of Aes from *E. coli* only preliminary X-ray data have been collected (*9*, *10*). On the other hand, we have recently studied the temperature- and denaturant-induced unfolding of thermophilic EST2 and hyperthermophilic AFEST (*11*−*13*).

In this paper we report the study of the urea- and GuHCl-induced unfolding of Aes and its single point mutant V20D-Aes, carried out by means of circular dichroism and fluorescence measurements. The unfolding transition of Aes proved to be more complex than the two-state $N \rightleftarrows D$ model, used to describe the behavior of the thermostable homologous enzymes (*11*−*13*), for the presence of an intermediate species that is not a molten globule. Experimental data suggest that the structure of Aes consists of two domains whose unfolding transitions are more or less independent depending on the denaturant used. A 3D model of the Aes structure, constructed by homology modeling using the structure of BFAE as a template, seems to support the reliability of this suggestion.

MATERIALS AND METHODS

Protein Purification and Sample Preparation. Recombinant Aes and a mutated version, V20D-Aes, obtained "by chance" during cloning of the *ybaC* gene, were overexpressed in *E. coli* and purified as previously described (*5*). The purity of homogeneous preparations was checked by SDS−PAGE and reversed-phase HPLC. Protein samples were dialyzed against appropriate buffers and concentrated by using an Amicon ultrafiltration apparatus for the following analyses.

Aes and V20D-Aes were dissolved in a 20 mM sodium phosphate buffer at pH 7.5, and the concentration was determined spectrophotometrically using a theoretical, sequence-based (*14*) extinction coefficient of 54500 M^{-1} cm^{-1} at 280 nm. Urea was used after recrystallization from ethanol/water (1:1) mixtures. Urea solutions were prepared fresh daily in buffered solutions, and the concentration of the urea stock solution was determined by refractive index measurements (*15*). A commercial 8 M solution from Sigma was used for GuHCl. Protein solutions for CD measurements were exhaustively dialyzed by using Spectra Por MW 15000−17000 membranes against buffer solution at 4 °C. The water used for buffer and sample solutions was doubly distilled. The pH was measured at 25 °C with a Radiometer pH meter, model PHM93.

† This work was supported by grants from the Italian Ministry for Instruction, University and Research (MIUR, Rome).

* To whom correspondence should be addressed. Phone: +39/081/674255. Fax: +39/081/674257. E-mail: delvecchio@chemistry.unina.it.

‡ University of Naples "Federico II".

§ University of Sannio.

|| CNR.

[1] Abbreviations: Aes, acetyl-esterase from *Escherichia coli*; AFEST, esterase from *Archeoglobus fulgidus*; EST2, esterase from *Alicyclobacillus acidocaldarius*; BFAE, brefeldine esterase from *Bacillus subtilis*; GuHCl, guanidine hydrochloride; HSL family, hormone-sensitive lipase family of the esterase/lipase superfamily; CD, circular dichroism; HPLC, high-performance liquid chromatography; SDS−PAGE, sodium dodecyl sulfate−polyacrylamide gel electrophoresis.

10.1021/bi048344f CCC: $27.50 © 2004 American Chemical Society
Published on Web 10/28/2004

Stock protein solutions were prepared in the buffer solution to be 10 times the requisite final protein concentration. Buffer, urea stock solution, and 10−20 μL of protein stock solution to give a final volume of 0.5 mL were added to 1 mL siliconized Eppendorf tubes. This yielded final urea concentrations from 0 to 9 M, GuHCl concentrations from 0 to 6 M, and the desired final protein concentration. Since high urea or GuHCl concentrations change the pH, the final pH for each sample was corrected by addition of HCl or NaOH. Each sample was mixed by vortexing and was incubated overnight at 4 °C. Longer incubation times produced identical CD signals.

Circular Dichroism. CD spectra were recorded with a Jasco J-715 spectropolarimeter equipped with a Peltier-type temperature control system (model PTC-348WI). The instrument was calibrated with an aqueous solution of D-10-(+)-camphorsulfonic acid at 290 nm (*16*). The molar ellipticity per mean residue, $[\theta]$ (deg cm^2 dmol^{-1}), was calculated from the equation $[\theta] = [\theta]_{obs}(mrw)/10lC$, where $[\theta]_{obs}$ is the ellipticity (deg), mrw is the mean residue molecular weight, 113, C is the protein concentration (g mL^{-1}), and l is the optical path length of the cell (cm). Cells with 0.2 and 1 cm path lengths and protein concentrations of about 0.1 and 1 mg mL^{-1} were used in the far- and near-UV regions, respectively. CD spectra were recorded with a time constant of 16 s, a 2 nm bandwidth, and a scan rate of 5 nm min^{-1}, signal-averaged over at least five scans, and baseline corrected by subtracting a buffer spectrum. The urea- or GuHCl-induced denaturation curves at constant temperature were obtained by recording the CD signal at 222 nm for each independent sample.

Fluorescence Measurements. Steady-state fluorescence measurements were performed with a JASCO FP-750 spectrofluorimeter equipped with thermostated cell holders, and temperature was kept constant by a circulating water bath. The protein concentration was 0.1−0.15 mg mL^{-1}. The excitation wavelength was set at 280 nm to include the contribution of Tyr residues to the overall fluorescence emission. The experiments were performed at 20 °C by using a 1 cm sealed cell and a 5 nm emission slit width and corrected for background signal. Both the change in fluorescence intensity and the shift in the fluorescence maximum wavelength were recorded to monitor the unfolding transition.

The binding of 1-anilinonaphthalene-8-sulfonate, ANS, to Aes was determined as a function of GuHCl concentation, by recording the fluorescence emission at 495 nm, upon excitation at 360 nm. The concentrations of Aes and ANS were 1 and 200 μM, respectively.

Homology Modeling. Aes and BFAE sequence alignment was obtained by using the Clustal W program (*17*) and refined manually using as a guide a secondary-structure prediction for Aes (PHD program). Gaps were reduced to a minimum and not allowed inside the structural elements. Molecular modeling was performed on a Silicon Graphics O2 workstation using the commercial software package Insight II (*Insight II user guide*; Biosym/MSI: San Diego, CA, October 1995). The high-resolution X-ray crystal structure of BFAE was used as a template. Several 3D models were constructed using the Modeller module (*18*) within Insight II. The methodology is based on satisfaction of spatial restraints that are obtained from an alignment of a target sequence with related 3D structures at high resolution (1.8−2.4 Å), using a conjugate gradient and a molecular dynamics simulated annealing as optimization procedures. Loops without reference in BFAE were subjected to further refinement in the program. The resulting models were verified using the on-line software WHAT IF, ERRAT, and VERIFY 3D on the Structure Analysis and Verification Server at http://shannon.mbi.ucla.edu/DOE/Services/SV/.

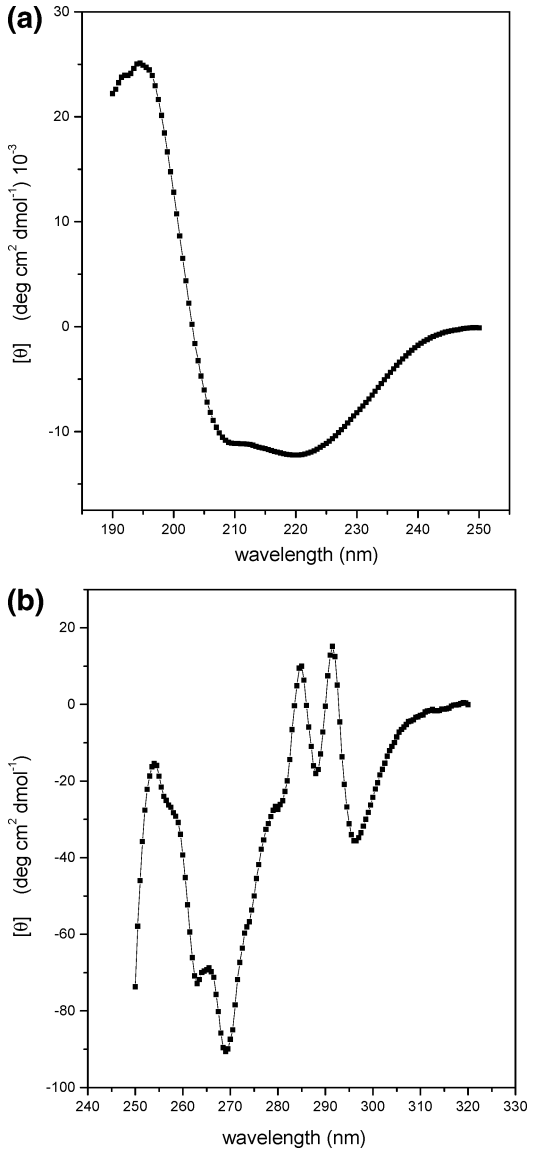

FIGURE 1: Far-UV (a) and near-UV (b) CD spectra of Aes recorded at pH 7.5 and 20 °C.

RESULTS

Stability of Aes against Chemical Denaturants. The far-UV (a) and near-UV (b) CD spectra of Aes at 20 °C in 20 mM phosphate buffer, pH 7.5, in Figure 1 show that the enzyme possesses a folded conformation in solution. Estimation of the secondary-structure content, performed by means of DICHROWEB (*19*), using the variable selection method (*20*), has given 38% α-helix, 22% β-sheet, 17% turns, and 23% unordered. Such values are close to those determined from the X-ray structures of other members of the HSL family, BFAE, EST2, and AFEST (*6*−*8*).

The fluorescence emission spectrum of Aes shows a maximum at 328 nm that, when the tertiary structure is

unfolded, shifts to 350 nm; the signal intensity decreases on increasing the denaturant concentration (not shown). Fluorescence spectra of proteins with a maximum around 330 nm are characteristic of Trp residues buried in the hydrophobic core, whereas fluorescence spectra with a maximum around 350 nm are characteristic of Trp residues exposed to the aqueous solvent (*21*). Therefore, since Aes has five Trp residues located all along the sequence, most of their side chains should be buried in the native structure, but well exposed to the aqueous solvent in the denaturant-induced unfolded state.

Urea- and GuHCl-induced unfolding of Aes was investigated by recording (a) the molar ellipticity at 222 nm, (b) the change in fluorescence intensity at 328 nm, and (c) the shift in the wavelength corresponding to the maximum of the fluorescence emission spectrum as a function of denaturant concentration. The measurements were performed at 20 °C, 20 mM phosphate buffer, pH 7.5, after an overnight incubation of the samples at 4 °C (longer incubation times gave rise to identical signals) and proved to be independent of protein concentration in the range 0.5−0.05 mg mL^{-1}.

With both urea and GuHCl the unfolding of Aes proved to be a reversible process: renaturation of completely unfolded samples upon suitable dilution showed a full recovery of all the spectroscopic features of the native enzyme. In this respect it has to be noted that Aes possesses nine Cys residues, only six of which are engaged in disulfide bridges on the basis of the structural model (see below). The three free sulfhydryl groups in the presence of urea or GuHCl do not impair the correct refolding of the polypeptide chain.

The urea-induced transition curves are shown in Figure 2. They have a sigmoidal shape, and the urea concentration at half-completion of the transition, $[urea]_{1/2}$, is 6.2 M, regardless of the spectroscopic probe used to monitor unfolding. This finding could be considered an indication that the urea-induced unfolding of Aes is a two-state N ⇄ D transition, as already found for EST2 and AFEST (*11*−*13*).

The GuHCl-induced transition curves, shown in Figure 3, have a more complex shape: two inflection points are present at 1.4 and 3.1 M GuHCl, respectively, regardless of the spectroscopic probe recorded to monitor the unfolding, suggesting the presence of an intermediate in equilibrium with native and unfolded Aes. To try to shed light on this unexpected finding, we studied the fluorescence intensity of ANS in the presence of Aes as a function of GuHCl concentration. It is firmly established that ANS increases its fluorescence intensity on binding to hydrophobic patches of proteins (*22*). This occurs upon the exposure of hydrophobic clusters to water as in the case of the formation of a molten globule intermediate (*23*). The experimental results, shown in Figure 4, demonstrate that no remarkable increase in the fluorescence intensity of ANS occurs, excluding the formation of a molten globule intermediate in the GuHCl-induced unfolding of Aes.

The strong difference in denaturing action of urea and GuHCl on Aes might be ascribed to the ionic character of GuHCl. To try to mimic the screening effect of charge−charge interactions exerted by GuHCl, we have recorded several urea-induced unfolding curves of Aes in the presence of different concentrations of NaCl. The latter is not a denaturing agent of globular proteins, but the presence of

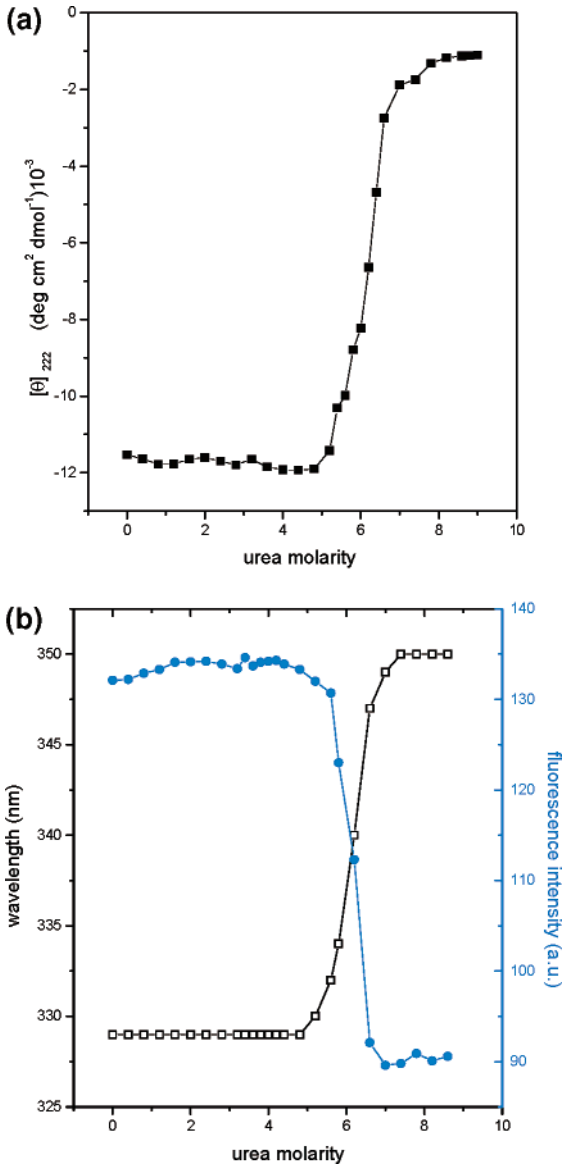

FIGURE 2: Urea-induced transition curves of Aes at pH 7.5 and 20 °C recorded by CD measurements at 222 nm (a) and fluorescence measurements (b). The continuous lines are meant only to guide the eye.

sodium and chloride ions in aqueous solution should cause a general screening effect of favorably electrostatic interactions among charged groups on the protein surface. The urea-induced unfolding curves of Aes in the absence of NaCl and in the presence of 1 M NaCl are shown in Figure 5; the unfolding is reversible also in the presence of NaCl. As expected, on passing from no NaCl to 1 M NaCl, the $[urea]_{1/2}$ value decreases from 6.2 to 5.2 M. The destabilizing effect caused by NaCl is reduced on further increasing the salt concentration: at 2 and 3 M NaCl the $[urea]_{1/2}$ values become 5.4 and 5.8 M, respectively. However, it is worth noting that all the urea-induced unfolding curves of Aes in the presence of different NaCl concentrations present a single inflection point. This means that the combined denaturing action of urea and NaCl is not able to reproduce the denaturing action of GuHCl on Aes. In all probability this is because the guanidinium ion, in contrast to the sodium ion, binds preferentially to exposed groups of the protein, causing a marked weakening of the electrostatic interactions among

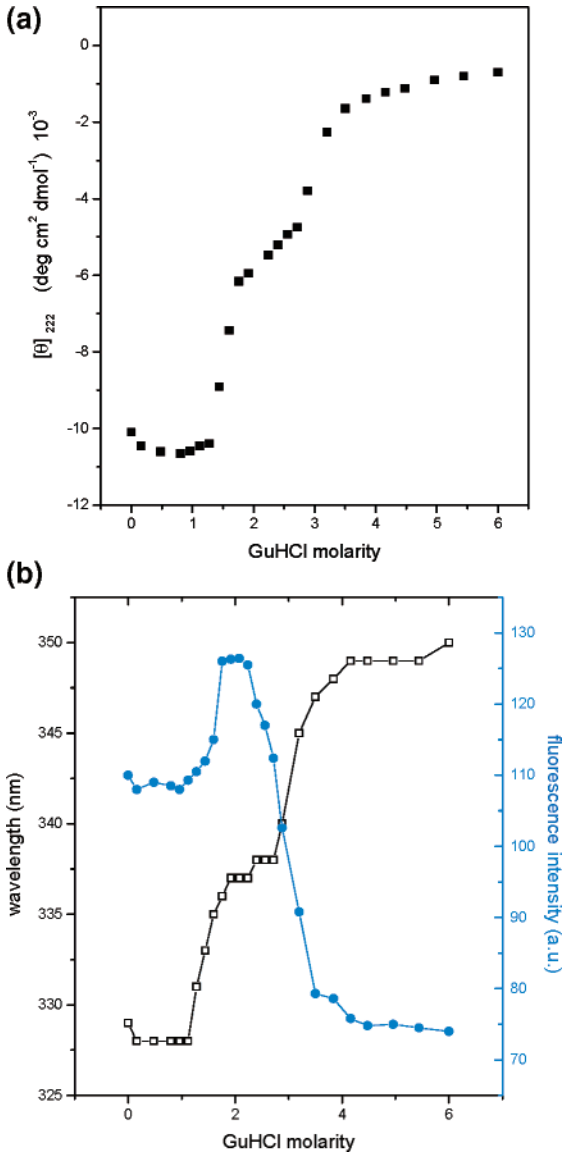

FIGURE 3: GuHCl-induced transition curves of Aes at pH 7.5 and 20 °C recorded by CD measurements at 222 nm (a) and fluorescence measurements (b). The continuous lines are meant only to guide the eye.

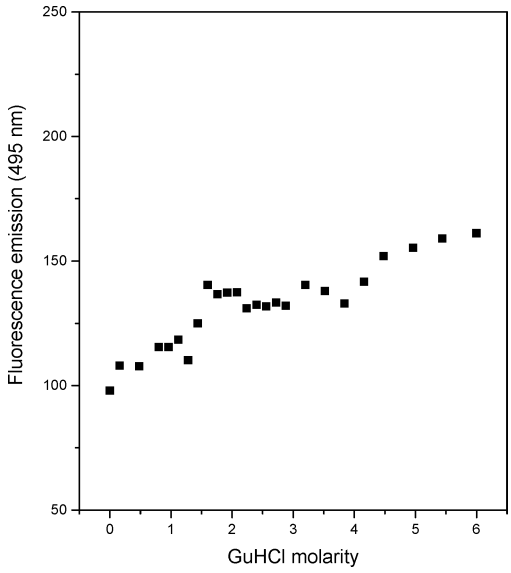

FIGURE 4: Binding of ANS to Aes as a function of GuHCl concentration. The fluorescence emission at 495 nm, upon excitation at 360 nm, was recorded at 20 °C.

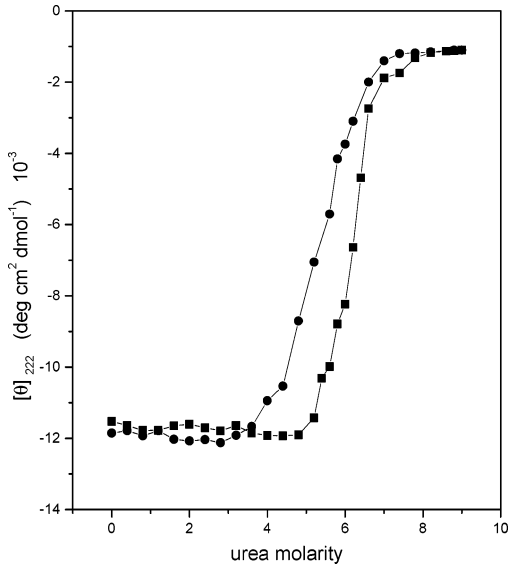

FIGURE 5: Urea-induced transition curves of Aes at pH 7.5 and 20 °C recorded by CD in the absence (square) and presence (circle) of 1 M NaCl.

the charged networks on the protein surface (*24*). Therefore, urea-induced unfolding curves of Aes in the presence of different NaCl concentrations indicate unequivocally that (a) the conformational stability of Aes depends on the ionic strength of the aqueous solution, suggesting that electrostatic interactions play an important role, and (b) the denaturing action of GuHCl cannot be mimicked by the combined action of urea and NaCl.

Stability of V20D-Aes. To further clarify the matter, we have investigated the consequences of a single point mutation, namely, V20D, on the stability of Aes against urea and GuHCl. The V20D mutation was obtained by chance during the cloning of the *ybaC* gene and was considered worth investigation because the substitution at position 20 of the nonpolar side chain of Val with the charged side chain of Asp might produce a marked effect. The far-UV and near-UV CD spectra of V20D-Aes in 20 mM phosphate buffer, pH 7.5, at 20 °C, were found identical to those of the parent protein (not shown), indicating that the secondary and tertiary structures of Aes were not influenced by the V20D single point mutation. Nevertheless, the urea- and GuHCl-induced unfolding curves of V20D-Aes, obtained by means of CD and fluorescence measurements (see Figures 6 and 7), are characterized by two inflection points: at 3.8 and 6 M urea, and at 0.8 and 2.5 M GuHCl (see Table 1). Thus, V20D-Aes shows complex unfolding curves against both urea and GuHCl: (a) the first inflection point at 3.8 M urea is not present in the case of Aes, whereas it is shifted from 1.4 to 0.8 M GuHCl as a consequence of the mutation; (b) the second inflection point occurs at a slightly lower denaturant concentration with respect to that found for Aes, 6 M urea versus 6.2 M urea, and 2.5 M GuHCl versus 3.1 M GuHCl, respectively.

These findings indicate that (a) the urea- and GuHCl-induced unfolding curves of Aes and its variant form cannot, in general, be described by the two-state N $\rightleftarrows$ D transition model and (b) the V20D mutation has important consequences on the conformational stability of Aes. A possibility

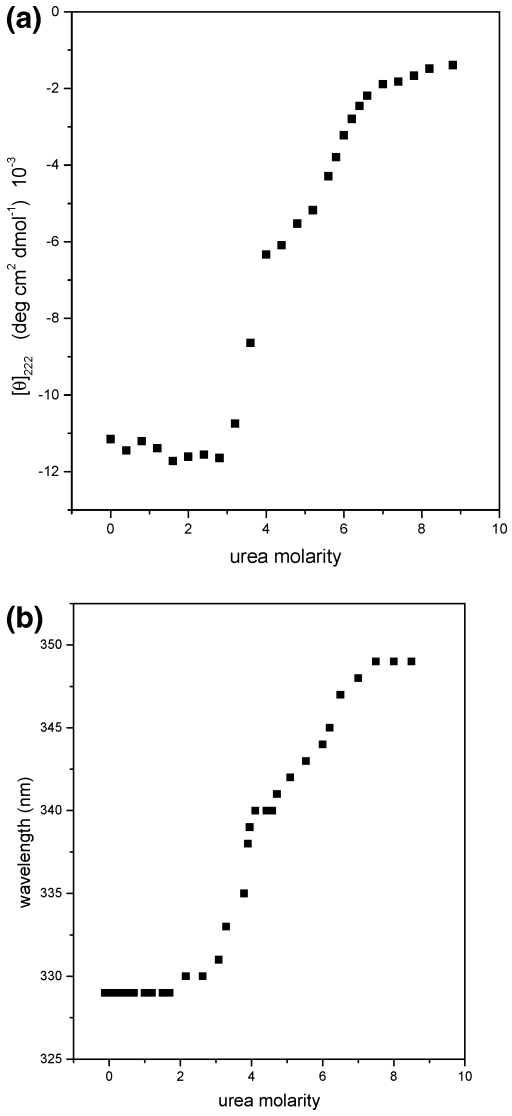

FIGURE 6: Urea-induced transition curves of V20D-Aes at pH 7.5 and 20 °C recorded by CD measurements at 222 nm (a) and fluorescence measurements (b).

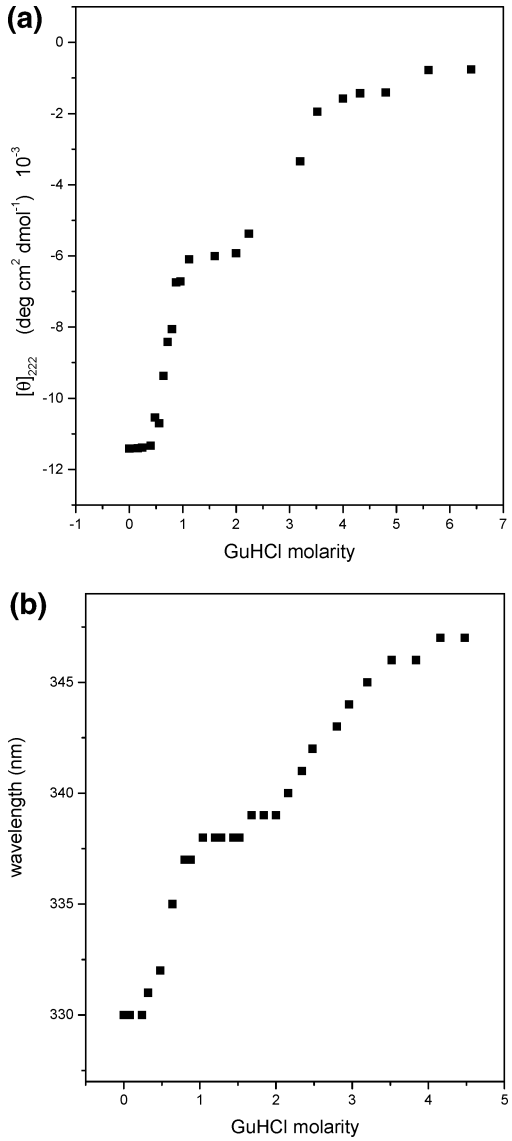

FIGURE 7: GuHCl-induced transition curves of V20D-Aes at pH 7.5 and 20 °C recorded by CD measurements at 222 nm (a) and fluorescence measurements (b).

is that Aes possesses two domains that unfold more or less independently. This hypothesis seems to be supported by inspection of the determined X-ray structures of some members of the HSL family (*8*), indicating the existence of a structural domain, mainly constituted by the N-terminal region, that covers and protects the active site region. It appears that (a) the V20D mutation causes the weakening of intraprotein interactions that are important for coupling together the two domains and (b) this weakening affects more significantly the stability of the less stable of the two domains.

Homology Modeling. To try to verify the existence of two structural domains in Aes and to try to rationalize the consequences of the V20D mutation, a molecular model of the enzyme has been constructed. Aes shows an amino acid sequence identity of (a) 25.3% with BFEA in a 245 amino acid overlap, (b) 29.3% with EST2 in a 232 amino acid overlap, and (c) 31.3% with AFEST in a 252 amino acid overlap (*10*). A previous model of Aes was obtained by using as a template the EST2 structure (*7*); in that model part of the Aes N-terminal sequence was not included, being longer than the EST2 sequence and highly divergent. Because the sequence of brefeldine esterase is longer than that of Aes, we attempted to model Aes on the known BFAE structure (PDB code 1JKM). We generated a secondary-structure-driven sequence alignment between Aes and BFAE (not shown), and submitted this alignment to the modeling procedure described in the Materials and Methods. Figure 8A shows the general folding pattern of the best Aes model obtained. The superimposed backbone traces of Aes and BFAE (Figure 8B) displayed a 0.82 Å RMS deviation on 273 Cα atoms, using a 2.75 Å cutoff distance. In a global

Table 1: Inflection Points Determined from the Urea- and GuHCl-Induced Transition Curves of Aes and V20D-Aes Monitored by Means of CD and Fluorescence Measurements at pH 7.5 and 20 °C

	probe	$[urea]_{1/2}$ (M)	$[GuHCl]_{1/2}$ (M)
Aes	$[\theta]_{222}$	6.2	1.5, 3.0
	I_{328}	6.2	1.4, 3.1
	λ_{max}	6.2	1.4, 3.1
V20D-Aes	$[\theta]_{222}$	3.6, 5.7	0.8, 2.5
	λ_{max}	3.8, 6.0	0.8, 2.5

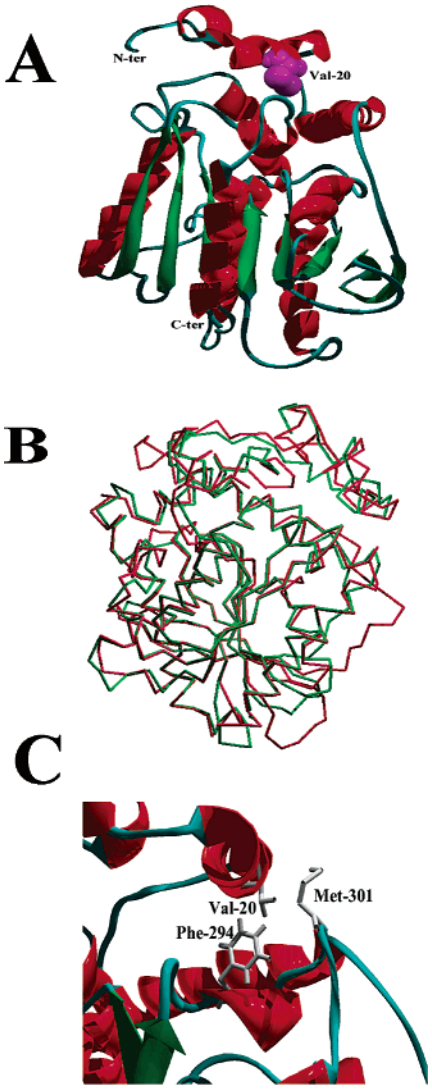

FIGURE 8: (A) Structural model of Aes. Strands are in green and helices in red. Val20 is shown as a van der Waals surface. (B) Superimposition between Cα traces of Aes (green) and BFAE (red). (C) Close view of the Val20 environment. The side chains of Phe294 and Met301 are shown in stick representation. The figures were generated with Swiss PDB viewer and rendered with POV3.1 for Windows.

superimposition (313 Cα atoms) the RMS deviation was 2.08 Å. The Ramachandran plot (not shown) indicates that most (98%) of the residues have ϕ and ψ angles in the core and allowed regions. The putative nucleophile Ser165 displayed anomalous ϕ and ψ angles, as expected (*8*). Most of the bond lengths, bond angles, and torsion angles evaluated with the WHAT IF program were in the range of values expected for a folded protein (data not shown). The structural model, shown in Figure 8A, corresponds to the canonical α/β fold (*25*), with one β-sheet made up of eight β-strands ($\beta1-\beta8$) twisted by about 90°. The identified strands were $\beta1$ (Arg61−Thr67), $\beta2$ (Gly70−Phe77), $\beta3$ (Leu87−Leu90), $\beta4$ (Thr117−Asp122), $\beta5$ (Gly160−Gly163), $\beta6$ (Val191−Tyr195), $\beta7$ (Pro253−Glu260), and $\beta8$ (Pro281−Tyr287).

It is important to note that the model suggests the existence of a structural domain, mainly composed by the N-terminal region of Aes, that covers and protects the active site of the enzyme. This N-terminal domain consists of about 50 residues and contains 3 α-helical stretches. Since the existence of this structural domain has already been identified in BFAE and AFEST (*8*), and since the N-terminal region of Aes is longer than that of AFEST, the presence of this structural domain in Aes should be considered reliable.

In addition, inspection of the model (Figure 8C) indicates that the side chain of Val20 is not exposed to the solvent, but interacts through nonpolar contacts with the side chains of Met301 and Phe294. These interactions seem to play a role in fixing the N-terminal region to the rest of the structure. Then, it is reliable that the V20D mutation, by introducing a negative charge in a hydrophobic environment, causes a destabilization of the local structure, which, in turn, causes a weakening of the coupling between the two structural domains of Aes.

DISCUSSION

Aes from *E. coli* should be considered the mesophilic counterpart of the thermophilic EST2 from *A. acidocaldarius* and the hyperthermophilic AFEST from *A. fulgidus*, whose conformational stability has already been investigated in our laboratories (*11*−*13*). Notwithstanding the difference in optimal growth temperature for the three source microorganisms, 37, 65, and 83 °C, respectively (*3*), the resistance to the denaturing action of urea is similar for the three esterases: $[\text{urea}]_{1/2} = 6.2$ M for Aes, 5.9 M for EST2, and 7.1 M for AFEST. This finding indicates that the resistance to high temperature does not correlate with the resistance against the action of urea. In addition, the behavior of Aes toward the denaturing action of GuHCl is very different from that of EST 2 and AFEST because its unfolding is characterized by two inflection points at 1.4 and 3.1 M GuHCl, whereas EST2 and AFEST show a single inflection point at 1.9 and 2.0 M GuHCl, respectively. These data point out that urea and GuHCl unfold Aes by means of a different molecular mechanism.

In this respect it is worth noting that we provide solely the values of the denaturant concentration at the midpoint of the transition curve. This choice is due to the fact that the application of the linear extrapolation model, LEM, and the denaturant binding model, DBM, to fit the transition curves of EST2 and AFEST, provided scattered results and no more insight into the physical origin of the resistance to denaturants of the two proteins (*11*). On these grounds, we proposed that the value of the denaturant concentration at the midpoint of the transition curve, the real experimental datum, is the correct parameter to characterize the stability of a protein against a chemical denaturant (*12*). The LEM model is a well-established method to describe the equilibrium stability of globular proteins against denaturants, because it has been found that the unfolding Gibbs energy change depends linearly on denaturant concentration (*15*). However, such linear dependence cannot provide molecular details on the action of chemical denaturants. In fact, several workers are trying to develop statistical mechanical approaches taking into account both the excluded volume effect and the contact interactions (*26*, *27*).

From the crystal structures of EST2 and AFEST it was determined that 39 and 42, respectively, ion pairs were present on the protein surface, using a cutoff distance of 6 Å (*12*). By taking into account that EST2 contains 41 acidic and 28 basic residues while AFEST contains 46 acidic and

34 basic residues, we suggested that the optimization of electrostatic interactions on the protein surface is a key factor for the high thermal stability of these two esterases (*12*). A similar analysis cannot be accomplished for Aes due to the lack of its crystal structure. However, since Aes contains a smaller number of charged residues, 38 acidic and 26 basic, with respect to EST2 and AFEST, we might suggest that the electrostatic interactions on the Aes surface are not optimized as well as in the two thermophilic enzymes.

To gain more information on the conformational stability of Aes, we have investigated the fluorescence intensity of ANS in the presence of the protein on increasing the GuHCl concentration. These measurements ruled out the existence of a molten globule intermediate in the Aes unfolding induced by GuHCl. In addition, we have shown that the combined action of urea and NaCl does not give rise to unfolding curves with two inflection points, as those produced by the GuHCl action. This implies that the denaturing mechanism of GuHCl cannot be reproduced by adding NaCl to aqueous urea solutions.

The understanding of the conformational stability of Aes has greatly benefited from the investigation of a variant form presenting a single point mutation, V20D-Aes. Even though this mutant form showed the same far-UV and near-UV CD spectra and fluorescence features as the parent protein, its unfolding curves present two inflection points regardless of the use of urea or GuHCl as chemical denaturant.

All these findings suggest the existence of two structural domains in Aes, whose coupling interactions are weakened by the V20D mutation. The construction of a structural model for Aes, using as a template the X-ray structure of BFAE, supports the above suggestion. In fact, the structure of Aes should consist of the classical α/β fold and of a further domain constituted by the N-terminal region of the chain. The elucidation of the X-ray structure of Aes, which is in progress (*9*, *10*), should be an important step in the full rationalization of the results presented in this work.

REFERENCES

1. Peist, R., Koch, A., Bolek, P., Sewitz, S., Kolbus, T., and Boos, W. (1997) Characterization of the aes gene of Escherichia coli encoding an enzyme with esterase activity, *J. Bacteriol. 179*, 7679−7686.
2. Kanaya, T., Koyanagi, E., and Kanaya, X. (1998) An esterase from Escherichia coli with a sequence similarity to hormone-sensitive lipase, *Biochem. J. 332*, 75−80.
3. Manco, G., Febbraio, F., and Rossi, M. (1998) in *Stability and Stabilization of Biocatalysts* (Ballesteros, A., Plou, F. J., Iborra, J. L., and Halling, P. J., Eds.) pp 325−330, Elsevier, Amsterdam.
4. Panagiatodis, C. H., Boos, W., and Shuman H. A. (1998) The ATP-binding cassette subunit of the maltose transporter MalK antagonizes MalT, the activator of the Escherichia coli mal regulon, *Mol. Microbiol. 30*, 535−546.
5. Mandrich, L., Caputo, E., Martin, B. M., Rossi, M., and Manco, G. (2002) The Aes protein and the monomeric alpha-galactosidase from Escherichia coli form a non-covalent complex. Implications for the regulation of carbohydrate metabolism, *J. Biol. Chem. 277*, 48241−48247.
6. Wei, Y., Contreras, J. A., Sheffield, P., Osterlund, T., Derewenda, U., Kneusel, R. E., Matern, U., Holm, C., Derewenda, Z. S. (1999) Crystal structure of brefeldin A esterase, a bacterial homolog of the mammalian hormone-sensitive lipase, *Nat. Struct. Biol. 6*, 340−345.
7. De Simone, G., Galdiero, S., Manco, G., Lang, D., Rossi, M., and Pedone, C. (2000) A snapshot of a transition state analogue of a novel thermophilic esterase belonging to the subfamily of mammalian hormone-sensitive lipase, *J. Mol. Biol. 303*, 761−771.
8. De Simone, G., Menchise, V., Manco, G., Mandrich, L., Sorrentino, L., Lang, D., Rossi, M., and Pedone, C. (2001) The crystal structure of a hyper-thermophilic carboxylesterase from the archaeon Archaeoglobus fulgidus, *J. Mol. Biol. 314*, 507−518.
9. Sorrentino, N., De Simone, G., Menchise, V., Mandrich, L., Rossi, M., Manco, G., and Pedone, C. (2003) Crystallization and preliminary X-ray diffraction studies of Aes acetyl-esterase from Escherichia coli, *Acta Crystallogr., D: Biol. Crystallogr. 59*, 1846−1848.
10. Gerber, K., Schiefner, A., Seige, P., Deiderichs, K., Boos, W., Welte, W. (2004) Crystallization and preliminary X-ray analysis of Aes, an acetyl-esterase from Escherichia coli, *Acta Crystallogr., D: Biol. Crystallogr. 60*, 531−533.
11. Del Vecchio, P., Graziano, G., Granata, V., Barone, G., Mandrich, L., Manco, G., and Rossi, M. (2002) Temperature- and denaturant-induced unfolding of two thermophilic esterases, *Biochemistry 41*, 1364−1371.
12. Del Vecchio, P., Graziano, G., Granata, V., Barone, G., Mandrich, L., Rossi, M., and Manco, G. (2002) Denaturing action of urea and guanidine hydrochloride towards two thermophilic esterases, *Biochem. J. 367*, 857−863.
13. Del Vecchio, P., Graziano, G., Granata, V., Barone, G., Mandrich, L., Rossi, M., and Manco, G. (2003) Effect of trifluoroethanol on the conformational stability of a hyperthermophilic esterase: a CD study, *Biophys. Chem. 104*, 407−415.
14. Gill, S. C., and von Hippel, P. H. (1989) Calculation of protein extinction coefficients from amino acid sequence data, *Anal. Biochem. 182*, 319−326.
15. Pace, C. N. (1986) Determination and analysis of urea and guanidine hydrochloride denaturation curves, *Methods Enzymol. 131*, 266−280.
16. Venyaminov, S. Y., and Yang, J. T. (1996) in *Circular Dichroism and the Conformational Analysis of Biomolecules* (Fasman, G. D., Ed.) pp 69−107, Plenum Press, New York.
17. Thompson, J. D., Higgins, D. G., Gibson, T. J. (1994) CLUSTAL W: improving the sensitivity of progressive multiple sequence alignment through sequence weighting, position-specific gap penalties and weight matrix choice, *Nucleic Acids Res. 22*, 4673−4680.
18. Sali, A., Pottertone, L., Yuan, F., van Vlijmen, H., Karplus, M. (1995) Evaluation of comparative protein modeling by MODELLER, *Proteins 23*, 318−326.
19. Lobley, A., Whitmore, L., and Wallace, B. A. (2002) DICHROWEB: an interactive website for the analysis of protein secondary structure from circular dichroism spectra, *Bioinformatics 18*, 211−212.
20. Johnson, W. C. (1985) Circular dichroism and its empirical application to biopolymers, *Methods Biochem. Anal.* 31, 61−163.
21. Lakowicz, J. R. (1983) *Principles of Fluorescence Spectroscopy*, Plenum Press, New York.
22. Semisotnov, G. V., Rodionova, N. A., Razgulyaev, O. I., Uverski, V. N., Gripas, A. F., and Gilmanshin, R. I. (1991) Study of the "molten globule" intermediate state in protein folding by a hydrophobic fluorescent probe, *Biopolymers 31*, 119−128.
23. Ptitsyn, O. (1995) Molten globule and protein folding, *Adv. Protein Chem. 47*, 83−229.
24. Perez-Jimenez, R., Godoy-Ruiz, R., Ibarra-Molero, B., Sanchez-Ruiz, J. M. (2004) The efficiency of different salts to screen charge interactions in proteins: a Hofmeister effect? *Biophys. J. 86*, 2414−2429.
25. Ollis, D. L., Cheah, E., Cygler, M., Dijkstra, B., Frolow, F., Franken, S. M. et al., (1992) The alpha/beta hydrolase fold, *Protein Eng. 5*, 197−211.
26. Schellman, J. A., (2003) Protein stability in mixed solvents: a balance of contact interaction and excluded volume, *Biophys. J. 85*, 108−125.
27. Saunders, A. J., Davis-Searles, P. R., Allen, D. L., Pielak, G. J., Erie, D. A. (2000) Osmolyte-induced changes in protein conformational equilibria, *Biopolymers*, *53*, 293−307.

BI048344F